Co-optimization of multi-energy system operation, district heating/cooling network and thermal comfort management for buildings

Co-optimization of Multi-Energy System operation, DHN/DCN and thermal comfort management for buildings

Lavinia Marina Paola Ghilardi[a], Alessandro Francesco Castelli[a], Luca Moretti[a], Mirko Morini[b], Emanuele Martelli[a,*]

[a] *Politecnico di Milano, Department of Energy, Via Lambruschini 4, Milano, 20154, Italy*

[b] *University of Parma, Department of Engineering and Architecture, Parco Area delle Scienze 181/a, Parma, 43125, Italy*

[*] *emanuele.martelli@polimi.it*

Abstract

The ongoing decarbonization of the energy sector spurs to employ distributed generation and efficient load control approaches (demand side management). This work tackles the optimal operation of a Multi Energy System (MES) and thermal comfort management for buildings with an integrated approach. The dynamic thermal energy balance of the buildings is included in the Mixed Integer Linear Programming (MILP) scheduling problem formulation, as to exploit the heat capacity of buildings and increase the operational flexibility of the generators. The method is firstly applied to a single building served by different energy systems comprising renewable energy sources. Then, the methodology is further extended by also integrating the model of the district heating/cooling network. This method is tested in a group of 12 buildings of the Campus of University of Parma, featuring different thermal properties. By enabling a variation within ± 2°C around the indoor temperature setpoint and by optimizing water delivery temperature, it is possible to achieve savings on operating costs over the baseline up to 80%. Results show that the load shift capability of buildings plays a major role when thermal demand mismatches RES availability or low electricity price periods. Moreover, DHN can be exploited as an additional short-term heat storage by varying water delivery temperature profile.

Keywords: Multi Energy Systems, demand-side management, MILP, district heating network

Parameters			
$c_{el,purch,t}$	Purchase electricity price	$q_{T,i}$	Machine OAT curve coefficient
$c_{el,sale,t}$	Sale electricity price	RU_i	Machine ramp-up limit
c_{fuel}	Fuel price	S_j	Surface covered by solar collectors
C_k	Building heat capacity	$T_{ext,t}$	Outdoor air temperature
$c_{O\&M}$	O&M cost	$T_{CIN,k,t}$	Outlet temperature of the hot fluid
c_w	water heat capacity	$T_{HIN,k,t}$	Inlet temperature of the hot fluid
D_p	Pipe diameter	$T_{m,i}$	Water average temperature of solar collectors
G_{nom}	Nominal solar irradiance of solar collectors	$T_{PD,k,t}$	Primary water delivery temperature
G_t	Solar irradiance	$T_{PD,user,k,t}$	Primary water delivery temperature (user side)
$k_{1,i}$	Machine part-load curve coefficient	$T_{PR,k,t}$	Primary water return temperature
$k_{2,i}$	Machine part-load curve coefficient	$T_{PR,user,k,t}$	Primary water return temperature (user side)
k_p	Pipe heat transfer coefficient	$T_{SD,k,t}$	Secondary water delivery temperature
$in_{max,i}$	Machine maximum power input	$T_{SD,user,k,t}$	Secondary water delivery temperature (user side)
$in_{min,i}$	Machine minimum power input	$T_{SR,k,t}$	Secondary water return temperature
$\dot{m}_{P,k}$	Mass flow rate of primary loop	$T_{SR,user,k,t}$	Secondary water return temperature (user side)
$\dot{m}_{S,k}$	Mass flow rate of secondary loop	$T_{UTA,t}$	Air forced ventilation temperature
$m_{T,i}$	Machine OAT curve coefficient	T_∞	Temperature of pipe surroundings
$mc_{p,nat,k}$	Air infiltration heat capacity	UA_k	Total thermal transmittance of the envelope
$mc_{p,for,k}$	Air forced ventilation heat capacity	Δt	MILP time discretization
$Q_{irr,k,t}$	Building solar gain	ε_k	Heat exchanger nominal effectiveness
$Q_{occ,k,t}$	Building internal gain	ρ_w	Water density

Abbreviations

AC	Absorption Chiller	HP	Heat Pump
B0	Building 0 (ref.)	ICE	Internal Combustion Engine
B1	Building 1 (higher heat capacity)	LP	Linear Programming
B2	Building 2 (higher glazed surface)	MILP	Mixed Integer Linear Programming
CC	Compression Chiller	MINLP	Mixed Integer Non Linear Programming
CCHP	Combined Cooling Heat and Power	NG	Natural Gas
CHP	Combined Heat and Power	OAT	Outdoor Air Temperature
DCN	District Cooling Network	O&M	Operation and Maintainance
DHN	District Heating Network	TCM	Thermal Comfort Management
DP	Dynamic Programming	RES	Renewable Energy Sources
FS	Fixed Setpoint	W1	Week 1 (winter)
GA	Genetic Algorithm	W2	Week 2 (spring)
HX	Heat Exchanger	W3	Week 3 (summer)

Sets		**Variables**	
$\mathcal{M}$	Set of dispatchable units	$el_{purch,t}$	Electricity import from the grid
$\mathcal{ND}$	Set of non-dispatchable units	$el_{sale,t}$	Electricity export from the grid
$\mathcal{K}$	Set of buildings	$in_{i,t}$	Machine input consumption rate
$\mathcal{T}$	Set of timesteps	$p_{i,t}$	Machine output production rate
Indexes		$Q_{k,t}$	Heat supplied to the building
i	Generator	$T_{k,t}$	Building indoor temperature
k	Building	$z_{i,t}$	Binary commitment variable
t	Timestep	$\Delta_{i,t}$	Binary start-up variable

1. Introduction

The energy transition towards more sustainable solutions requires the coordinated management of different energy resources and loads. Multi-energy systems (MESs) are considered a favourable route to integrate various energy vectors and activate synergies among them. MESs are *multi-service* and *multi-fuel* systems [1], where heat, cold, electricity and fuels interact with each other at different levels. They allow to achieve better performances compared to "traditional" systems, both from the environmental, technical and economic point of view [1]. Local energy production has to cope with the fluctuating availability of RES (Renewable Energy Sources) and therefore the need for flexible solutions is to be advocated. In this framework, the building sector represents a great opportunity, as thermal mass - readily available - can be exploited to shift thermal

loads. Moreover, buildings represent a large fraction of final energy consumption, around 40% in Europe and 32% globally [2]. More specifically, heating and cooling needs account for 55% and 30% of buildings energy consumption in EU, respectively in residential and in commercial sector [2].

Due to the multiple possible synergies between the installed units and the large number of degree of freedom (units loads, units on/off and energy storage management), the operation of MESs calls for the development of systematic optimization approaches. From a mathematical point of view, the operation optimization problems can be formulated rigorously as nonconvex Mixed Integer Non Linear Programming (MINLP) because of the nonlinear effects of part-load operation on generator efficiency [3] as well as possible non-isothermal mixing occurring in water headers [4]. The introduction of binary variables becomes fundamental when start-up/shut-down operation is included. Nevertheless, MINLP problems (especially if nonconvex) are more computationally demanding, require considerably more computational time and may fail to find a feasible solution [5][4]. As a result, several studies have proposed optimization approaches based on either Mixed Integer Linear Programming (MILP) formulations (e.g. Brahman et al.[6], Buoro et al. [7]), Dynamic Programming (e.g., Gambarotta et al. [8] and Marano et. al [9]) metaheuristic algorithms (e.g., the genetic algorithm of Fang and Lahdelma [10], the neurodynamic-based optimization algorithm by Huang et al. [11]) and distributed control algorithms (e.g., the double-newton descent algorithm by Yushuai et al. [12]). Among these, techniques based on MILP problem formulations appear to be the most promising due to the possibility of including all operational constraints (including ramping and start-up constraints), keep a good solution accuracy [4] [5] via proper linearization techniques, rely on very efficient commercially available MILP solvers (e.g., CPLEX , Gurobi) and feature global optimality guarantees on the obtained solution.

However, most literature addressing the optimization of MES considers the thermal demand profile of buildings as an exogenous input to be met. Examples are the work of Sandou et al.[13], Bischi et al. [3], Moretti et al. [4][14], Fang and Lahdelma [10] and Buoro et al. [7]. Sandou et al. [13] optimize the supply temperature and the scheduling of the units given a thermal input profile with Sequential Quadratic Programming (SQP), including constraints on heat exchangers of the DHN and thermal propagation delay in pipes. Bischi et al. [3] formulate the operational problem of the aggregated energy system as a MILP by adopting a piecewise linear approximation of the part-load performance maps of the units. Moretti et al. [14] extended the MILP to account for the uncertainty affecting the forecasts of heat and electricity demand as well as production from

renewable sources. Moretti at al. [4] further extend the MILP formulation to handle complex network arrangements with units generating hot water at different temperatures and stratified thermal storage systems. Fang and Lahdelma [10] develop a Genetic Algorithm to optimize the scheduling of distributed units, the delivery temperature and the mass flow rate of the DHN (District Heating Network), accounting for transport delay in pipes. Buoro et al. [7] formulate a multi-objective MILP to minimize total annual operating of a distributed cogeneration system with a solar thermal plant. Gambarotta et al. [8] develop a DP algorithm to minimize the overall primary energy consumption of many energy technologies serving a residential buildings, comprising photovoltaics panels (PV), thermal collectors, a micro gas turbine, heat pumps, an energy storage and a boiler. The thermal power profile supplied to the buildings is fixed (input profile) and not optimized. This decoupling between the building heat demand and the MES operation does not allow the possibility of exploiting the building thermal capacity as a storage system , as pointed out in [15]. For this reason, a few works incorporate the building model in the operational optimization problem. Darivianakis et al. [16] formulate a robust predictive control linear program and adopt a bi-linear state-space model of the building. Baader et al. [17] propose a MILP formulation for the scheduling problem, including a representation of closed-loop process dynamics. To this end, they discretize the single state grey-box model of the building via collocation polynomials. Brahman et al. [6] address the home scheduling problem of a residential building through a MILP formulation. They introduce binary variables to state the on/off status of the energy system and household appliances, which can be curtailed or shifted. The thermal demand of the building is regarded as a flexible and they include in the formulation the single-state grey box model of the building approximated to the forward difference. Nguyen and Le [18] tackle the LP home energy scheduling, by integrating a three state variables (air, envelope and internal mass temperature) model of the building. However, all these works neglect the transport dynamics of the pipes and the operation of heat exchanger of the district heating network. Guelpa et al. [19] aim at minimizing thermal peaks of a large scale district heating network with a Genetic Algorithm, by acting on the advanced start-up of the heating system. In order to reduce the degrees of freedom of the problem, they defined a-priori maximum anticipation for each building, by clustering them according to the parameter τ (the ratio of the thermal capacity to thermal conductivity). Gu et al [20] addresses the optimal scheduling of a CHP and a wind farm, embedding the dynamic model of the buildings and of heat transmission across the pipes in the formulation. They formulate the problem as a MINLP which however does not model the effect of the heat

transfer temperature difference in the heat exchangers. Table 1 summarizes the main approaches proposed in literature for optimizing the operation of MES and energy districts. s

Table 1– Main approaches for optimizing the operation of energy districts and multi energy systems.

Ref.	Optimization technique	Goal	Optimized variables	Key equations	Application	Advantages	Disadvantages
[13]	NLP	Control	Loads of units , DHN supply temperatures and opening degree valves of DHN	Thermal propagation delay in pipes, HX operation, aggregated production models	2 DHN rings with 6 consumers supplied by 2 aggregated production sites	Detailed DHN non-linear dynamics and heat exchangers operation	Heat capacity of buildings not exploited; aggregated model for production sites without considering units on/off operation
[3]	MILP	Operation	Scheduling of units (loads and on/off), management of heat storages	Linearized perfomance maps, energy balances, units technical limits	MES with combined cooling, heat and power	Computational load	Heat capacity of buildings not exploited; DHN dynamics not included
[4]	MINLP/ MILP	Operation	Scheduling of units, water mass flow rates and temperatures, management of thermocline	Linearized perfomance maps, energy and mass balances, units technical limits, non-isothermal mixing in headers	MES serving DHN	It accounts for different delivery temperatures of units and parallel/series connections	Heat capacity of buildings not exploited; more computational compared to energy flow models
[10]	Simulation-based optimization (GA + DHN simulation)	Operation	Supply temperatures and mass flow rates of DHN	Thermal propagation delay in pipes, non-isothermal mixing	Non-cyclic DHN with 3 consumers supplied by 2 plants	Detailed non-linear DHN dynamics and mixing	Heat capacity of buildings is not exploited; no optimality guarantee; no optimization of units operation
[19]	Simulation-based optimization (GA + DHN and building simulation)	Operation	Start-up time of the heating system	Clusterization of buildings, maximum anticipation constraint, thermal propagation delay in pipes, HX operation	Large scale DHN	No need for linearization; application to very large scale DHN	No optimality guarantee; no optimization of units operation

[20]	MINLP	Operation	Scheduling of units, supply temperatures of DHN, buildings indoor temperatures	Delay in pipes, non-isothermal mixing, performance maps of the units, single-state grey-box model of the buildings	Non-cyclic DHN with 24 thermal loads supplied by a CHP and a wind farm	Detailed non-linear DHN dynamics and mixing	No HX operation; no global optimality guarantees; computational load
[18]	LP	Control	Loads of units, buildings temperatures	Three-state grey-box model of the buildings, comfort constraints	Home energy management for residential buildings	Accuracy of the building model; computational load	No DHN dynamics and HX; performance maps and start-ups of the units not modelled; calibration of more parameters of the building
[15]	LP	Control	Load of units, buildings temperatures	Linearized bi-linear model of the buildings with states variables for every room, comfort constraints, linearized performance maps of units	Energy management control of aggregated buildings supplied by an energy hub	Accuracy of the building model; computational load	No DHN dynamics and HX; units on/off not optimized; calibration of more parameters of the building model
[6]	MILP	Operation	Scheduling of units, buildings indoor temperatures	Single-state grey-box model of the buildings, comfort constraints, loads modelling (shiftable, active, flexible)	Home energy scheduling of residential building with various type of loads	Computational load	No DHN dynamics and HX operation, performance maps of the units not modelled
[17]	MILP	Control	Scheduling of units, buildings indoor temperatures	Single-state grey-box model of the buildings, comfort constraints, linearized performance map of units	Energy management control of an office building supplied by a HP	Discretization with collocation polynomials	No DHN dynamics and HX operation
[21]	Dynamic Programming	Control	Water mass flow rate, mixing	Single-state grey-box model of the	DHN of a 2 buildings school complex	No need for linearization	Decoupled multi-agent approach

			temperature of DHN	buildings, delay in pipes, HX operation, non-isothermal mixing	supplied by a boiler		

Although considered state-of-the art optimization approaches for MES operation, none of the previously mentioned works formulates the combined optimization of MES scheduling (including on/off), DHN operation (including heat exchangers between primary and secondary loops) and thermal management of the buildings as a single Mixed Integer Linear Program (MILP). Compared to MINLP formulations, thanks to linearity of the problem and efficient commercially available solvers, MILP-based methods allows optimizing considerably longer time horizons and more complex systems (e.g., with more production units, buildings and branches of the DHN), as shown in [4] and [5]. This work aims at covering the above cited gap by proposing a novel MILP formulation including rigorously linearized models for the MES units, the dynamic thermal model of the building, and the dynamic thermal model of the DHN with related heat exchangers. The proposed MILP approach allows optimizing not only the operation of the MES units but also the profiles of DHN water delivery temperature, the thermal energy supplied to each building and the dynamic evolution of the indoor temperature. Compared to previous works based on MILP models (e.g., [3], [4], [12]), the flexibility provided by the heat capacity of the buildings allows for shifting energy consumption and a more economical operational planning for production units. The analysis is firstly conducted for single buildings for three representative weeks of the year, encompassing several MES designs and different thermal features of the building (thermal inertia and window surface). The model is also applied to the Campus of University of Parma, and the conventional management strategy, with given thermal profiles of buildings and of water supply temperature, is compared to the proposed "thermal comfort management" (TCM). Under the latter strategy, the energy service company requires the users a certain degree of flexibility, in terms of indoor temperature variations within a quality band, and the profile of water delivery temperature of DHN is optimized.

2. Methodology

2.1 Problem statement

The general representation of the energy district under consideration is provided in Figure 1. It consists of a centralized multi-energy system that provides various energy services to radially arranged buildings. Thermal energy is delivered to end users through a district heating network, with primary and secondary circuits and different sub-stations. The key elements of the operation planning problem for this system are provided in Table 2.

Table 2– Input data, decision variables, objective function and constraints of the optimal operation planning problem.

Data	**Decision variables**
Set of dispatchable generation units $\mathcal{M}$, with performance curves and technical limits	Scheduling and loads of dispatchable units
Set of non-dispatchable units $\mathcal{ND}$	Amount of non-dispatchable production to be curtailed
Set of buildings $\mathcal{K}$, with defined thermal parameters	Power exchanged with the grid
District heating (or cooling) network with radial topology, comprising a primary and a secondary loop with fixed mass flow rate	Heating or cooling power supplied to buildings
Forecasted electricity prices, electric demand profile and occupancy in buildings	Buildings indoor temperature
Forecasted outdoor air temperature and irradiance	Delivery and return temperatures of the primary and secondary circuits
Objective function	
Operating costs	
Main constraints	
Dynamic thermal balance of the building	Thermal comfort requirements
Heating, cooling and electric balances	Limits on heat transfer in heat exchangers
Technical limits of generating units	Thermal propagation delay in pipes of DHN

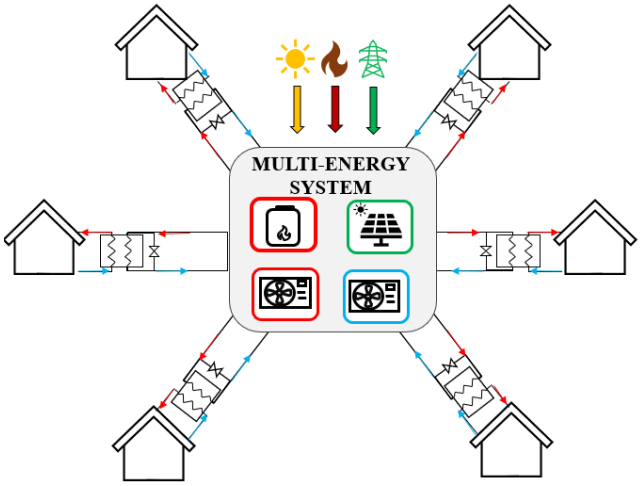

Figure 1– General scheme of an energy district served by a Multi Energy System (MES) with radial DHN.

2.2 Objective function

The MILP scheduling problem aims at minimizing total operating costs, which include the cost of the fuel c_{fuel} supplied to the generators $\mathcal{M}_{fuel}$, operation and maintenance costs of controllable units $\mathcal{M}$ and the net values of trades with the electric grid:

$$\sum_{t\in\mathcal{T}}\Big[\sum_{i\in\mathcal{M}_{fuel}} c_{fuel}\cdot in_{i,t} + \sum_{i\in\mathcal{M}} c_{OM,i}\cdot z_{i,t} + \left(c_{el,purch,t}\cdot el_{purch,t} - c_{el,sale,t}\cdot el_{sale,t}\right)\Big]\cdot\Delta t \quad \textbf{(1)}$$

Where: $c_{el,purch,t}$ and $c_{el,sale,t}$ are time-varying price profiles for the purchase and sale of electricity and Δt is the time discretization of the MILP. The variables involved in the objective function are the commitment binary variable of the generators $z_{i,t}$, the fuel input $in_{i,t}$ of the machines and the amount of electricity to be sold $el_{sale,t}$ or purchased $el_{purch,t}$ from the grid.

2.3 Controllable units

Electrical and thermal generators are classified on the basis of their controllability, where $\mathcal{M}$ denotes dispatchable units and $\mathcal{ND}$ non-dispatchable ones. Controllable units must operate in compliance with technical limitations, such as minimum and maximum load allowed (2) minimum uptime (3)
and ramp up limits RU_i at start-up (4)
.

$$z_{i,t} \cdot in_{min,i} \leq in_{i,t} \leq z_{i,t} \cdot in_{max,i}, \quad \forall i \in \mathcal{M}\ \forall t \tag{2}$$

$$z_{i,t} \geq z_{i,t} - z_{i,t-1} \quad \forall i \in \mathcal{M}, \forall t \in [1, T-m], \forall m \in [0, min_{UT}(i)/\Delta t] \tag{3}$$

$$in_{i,t} \leq \Delta_{i,t} \cdot RU_i + (1 - \Delta_{i,t}) \cdot in_{max,i} \forall i \in \mathcal{M} \forall t \tag{4}$$

Where: $z_{i,t}$ ·is the unit commitment variable and $\Delta_{i,t}$ is a binary variable to state whether the unit has been switched on at a given timestep. The variable $\Delta_{i,t}$, defined by a set of inequality constraints with respect to $\boldsymbol{z_{i,t}}$ [3], is essential for modelling the start-up penalty, which is regarded in this work as a reduction of the useful output of generators. In order to preserve model linearity, we linearized the part-load performance curves of the generating units, following the approach proposed by Zatti et al [22]. In this analysis, we overlooked the effect of DHN water delivery temperature variations on generators performance, but further extensions of the model could investigate the influence of this factor. Hence, the relationship between power output $p_{t,i}$ and power input $in_{t,i}$ is evaluated by Eq. (5)

.

$$p_{i,t} = k_{1,i} \cdot in_{i,t} + k_{2,i} \cdot z_{i,t} \tag{5}$$

Where the coefficients $k_{1,i}$ and $k_{2,i}$ are calculated with the best fit of data found in literature or commercially viable, with minor approximations (<5%). In particular, the coefficients of the heat pump and the boiler are directly derived from Zatti et al [22]. Meanwhile, the coefficients of the internal combustion engine are evaluated from [23], that of the compression chiller (CC) and the absorption chiller (AC) from respectively [24] and [25]. In the specific case of heat pumps and compression chillers, the effect of the outdoor air temperature is considered as a linear function whose value affect the different load rates independently [26]. For these units, the power output of Eq. (5) is multiplied to the following expression:

$$f_i(T_{ext}) = (m_{T,i} \cdot T_{ext} + q_{T,i}) \tag{6}$$

Where: m_T and q_T are calculated by fitting performance data found in [24] and [27]. The coefficients adopted for modelling off-design operation of generators are summarized in Table 3.

Table 3– Linearization coefficients for modelling energy generators performance curves

	Type	Output	$k_{1,i}$	$k_{2,i}$	$m_{T,i}$	$q_{T,i}$	Ref.
Boiler	NG	Heat	0.976	-0.032	-	-	[22]
HP	Air cooled	Heat	3.590	-0.080	0.019	0.805	[22] [27]
ICE	< 200 kWel (NG)	Electricity	0.442	-32.04	-	-	[28]
		Heat	0.469	10.37	-	-	
ICE	1500 - 4000 kWel (NG)	Electricity	0.490	-237.6	-	-	[22]
		Heat	0.439	-211.8	-	-	
CC	<150 kW_{cool} (Air cooled)	Cooling	3.467	-0.347	-0.041	2.435	[29] [26]
CC	700-1700 kW_{cool} (Air cooled)	Cooling	4.802	-1.402	-0.031	2.059	[29] [24]
AC	209-6138 kW_{cool} (Air cooled)	Cooling	0.76	0	-	-	[25]

2.4 Non-dispatchable units

The production rate of non-dispatchable units, namely photovoltaics panels and solar thermal collectors, is evaluated by functions of forecasted outdoor air temperature $T_{ext,t}$ and solar irradiance G_t as follows. The power output $p_{i,t}$ of the units depends on the efficiency $\eta_{i,t}$, the solar irradiance and the surface covered S_i, according to Eq. (7)

$$p_{i,t} = \eta_{i,t} \cdot G_t \cdot S_i \tag{7}$$

The efficiency of solar thermal collectors is computed via Eq. (8)

.

$$\eta_{ST,t} = \eta_{0,ST} - a_{1,ST} \cdot \frac{T_{m,ST} - T_{ext,t}}{G_{nom}} - a_{2,ST} \cdot \left(\frac{T_{m,ST} - T_{ext,t}}{G_{nom}}\right)^2 \tag{8}$$

Where: and G_{nom} state for nominal value of solar irradiance, while $\eta_{0,j}$, $a_{1,j}$ and $a_{2,j}$ are performance coefficients found in technical datasheet [30]. The mean water temperature across the collectors $T_{m,ST}$ is assumed to be constant over time, to guarantee a linear formulation suitable for the MILP model, and it is taken as equal to 50°C in the case

study. Given this low temperature, the heat produced by solar thermal collector is directly yielded to the secondary loop of the district heating network to pre-heat the water flowing in the sub-stations, as shown in Figure 2. In case of over-production, this heat can be dissipated to guarantee indoor thermal comfort to end users and to allow the feasibility of the model.

Meanwhile, the efficiency of photovoltaics panels depends on the efficiency $\eta_{0,\mathrm{PV}}$ in standard conditions (25°C, 1000 W/m^2, AM 1.5); the degradation temperature coefficient γ_T and on the operating temperature of the cell $T_{cell,t}$, following Eq. (9)

.

$$\eta_{PV,t} = \eta_{0,PV} \cdot \left(1 + \gamma_{PV} \cdot \left(T_{cell,t} - T_{ref}\right)\right) \tag{9}$$

The operating temperature of the cell is a function of outdoor air temperature and irradiance (see Eq. 2.10), by means of the parameters $NOCT$ (Nominal Operating Cell Temperature) G_{NOCT} and $T_{ref,NOCT}$.

$$T_{cell,t} = T_{ext,t} + \left(NOCT - T_{ref,NOCT}\right) \cdot \frac{G_t \cdot 1000}{G_{NOCT}} \tag{10}$$

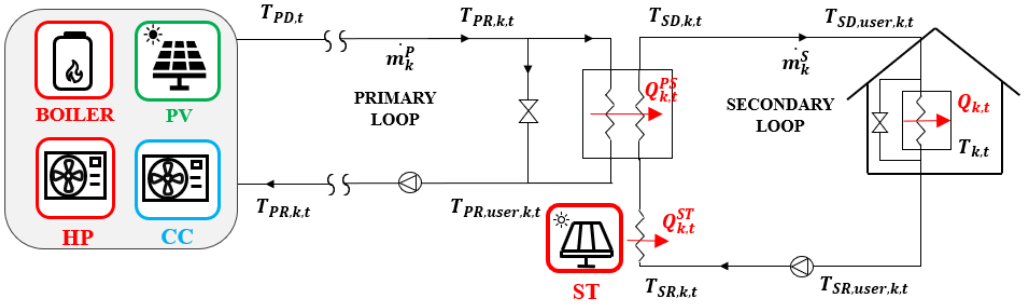

Figure 2 – General scheme of one branch of the DHN showing the primary loop.

2.5 Building model

Building simulation models can be classified into three categories: white-box, grey-box and black-box models. White-box models are physical-based approaches that describe in detail the complex energy dynamics of the system, black-box models are totally data-driven (e.g., sampled profiles used as input for a machine learning algorithm or a best fit function) and grey-box models combines the aspects of both. Simplified grey box models are the most suitable for optimization and operation control since they need relatively short computation time and a restricted number of parameters [31]. The model adopted

in this work is a single state grey-box, derived from Gambarotta et al. [32], where the coefficients are found trough best-fit of TRNSYS white-box model:

$$C_k \frac{dT_k}{dt} = UA_k \cdot (T_{ext,t} - T_{k,t}) + mc_{p,nat,k} \cdot (T_{ext,t} - T_{k,t}) + mc_{p,for,k} \cdot (T_{UTA,t} - T_{k,t}) + Q_{irr,k,t} + Q_{occ,k,t} + Q_{k,t} \quad (11)$$

Where: $T_{k,t}$ is indoor temperature, $T_{out,t}$ is outdoor air temperature, $T_{UTA,t}$ is the temperature of the air coming from the air treatment unit, C_k is the total thermal capacity of the building [kJ/°C], UA_k is the mean thermal transmittance of the envelope multiplied by its surface [kJ/h/°C], $mc_{p,nat,k}$ is the thermal capacity of the air infiltration [kJ/h/°C], $mc_{p,for,k}$ is the thermal capacity of the air forced ventilation [kJ/h/°C], $Q_{irr,k,t}$ and $Q_{occ,k,t}$ are respectively solar and internal gains, while $Q_{k,t}$ is heat supplied to end-users. In particular, $T_{k,t}$ and $Q_{k,t}$ are the variables to be optimized by the model, in compliance with comfort requirements. The differential equation is discretized using forward finite difference:

$$C_k \frac{T_{k,t+1} - T_{k,t}}{\Delta t} = UA_k \cdot (T_{ext,t} - T_{k,t}) + mc_{p,nat,k} \cdot (T_{ext,t} - T_{k,t}) + mc_{p,for,k} \cdot (T_{UTA,t} - T_{k,t}) + Q_{irr,k,t} + Q_{occ,k,t} + Q_{k,t} \quad (12)$$

We compared this approximated solution for different Δt values with the analytic one, found for some test input profiles of irradiance, occupancy and heat input. The absolute error in internal building temperature is below 0.1°C if Δt is lower than 15 minutes. This error has been considered sufficiently low for the purposes of the planning optimization and therefore this time discretization is used for single building case study. As it will be explained further, the choice of time discretization for the energy district case study was driven by the heat propagation delay in pipes (i.e. the time resolution has to be sufficiently tight to capture this phenomena within the model). For this reason, a time step of 7.5 minutes was adopted.

2.6 Building time constant $\boldsymbol{\tau}$

The general solution of the heat balance of the building (Eq. (13)without any thermal input (from the heating systems, internal or solar gains) can be written in the following form:

$$\theta = \theta_0 \cdot e^{-\frac{t}{\tau}} \quad (13)$$

Where θ is the difference between indoor temperature and external temperature at any time step, while θ_0 corresponds to this difference at the initial condition. Hence, the time constant τ is the ratio of the heat capacity to building dispersions coefficient and can be regarded as the time needed to the initial temperature difference θ_0 to be reduced by 63.2%. An understanding of this behaviour is provided by Figure 3, depicting the temperature profile of θ over the time of two buildings featuring a time constant of 34 hours and 158 hours, respectively. This time constant clearly plays a key role in the thermal dynamic behaviour of the building and the possibility of implementing thermal comfort management strategies.

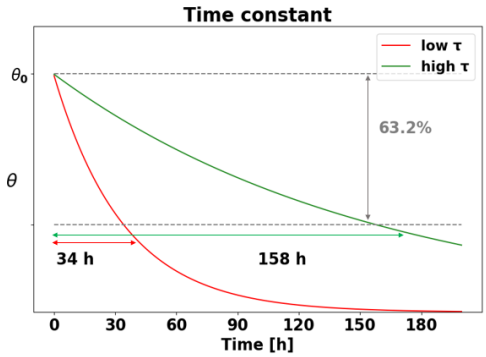

Figure 3 Temperature evolution of two buildings without additional thermal inputs (e.g. heating system, solar and internal gains), featuring a time constant of 34 h and 158 h.

2.7 District heating/cooling network model

The district heating/cooling network under consideration presents a radial topology with a centralized multi-energy system. The general representation of a branch of this network is depicted in Figure 2. Controllable thermal generators supply the primary loop, while the heat produced by solar thermal collectors (if present) is conveyed to the lower temperature secondary circuit to pre-heat the water. In the summer season, the network is used to transport cold water for cooling purposes.

The dynamic mathematical model of the DHN/DCN includes two types of constraints in order to address heat exchanger operation (Eq. (14)and (15)) and pipe thermal propagation delay (Eq. (16)), respectively. The main assumption of the model is that the DHN (or DCN) operates with constant mass flow rate, while water delivery temperature $T_p^p(t)$ (equal for all buildings) can be regulated. This is a typical regulation mode used in district heating systems [20]. The input thermal power of each building can be decreased by adjusting the bypass valve of the heat exchanger in the sub-station. This valve regulates the flow rate of the fluid with minimum heat capacity rate, which is assumed to be always on the same side of the heat exchanger. Notably, with the nominal temperature differences between delivery and return that occur in the case study (see Section 3), the fluid with minimum thermal capacity is on the primary side during heating season and on the secondary side during the cooling season. In order to guarantee this condition on minimum heat capacity rate, we introduced the constraint expressed by Eq. (14)

). Nevertheless, this constraint has proven to be non-binding in test cases.

$$\Delta T_{min} \geq \Delta T_{max} \tag{14}$$

Once the hypothesis on the minimum heat capacity rate is verified, the thermal power provided to each building k can be expressed as a linear function of the supply temperature of the DHN (see Eq. (15)).

$$Q(k,t) \leq \varepsilon_k \cdot c_w \cdot \dot{m}_{min,k} \cdot \left(T_{HIN,k,t} - T_{CIN,k,t}\right) \tag{15}$$

Where: ε_k is nominal effectiveness of the counter flow heat exchanger, c_w is heat capacity of water, $\dot{m}_{min,k}$ is the nominal mass flow rate of the fluid with minimum thermal capacity, $T_{HIN,k,t}$ is the inlet temperature of the hot fluid and $T_{CIN,k,t}$ is the inlet temperature of the cold fluid.

As for the delay in heat propagation:, we include a correlation between inlet T_t^{IN} and outlet T_t^{OUT} temperature of the pipes, following the approach proposed by Dobos et al. [33]. The solution of the energy conservation equation in the pipes can be written as Eq.(16), assuming one dimensional flow and disregarding heat capacity of pipes and heat conduction in the axial direction.

$$T_{OUT,t} = T_\infty + \left(T_{IN,t-1} - T_\infty\right) \cdot \left(1 - \frac{4 \cdot k_p}{D_p \cdot c_w \cdot \rho_w} \cdot \Delta t\right) \tag{16}$$

Where: Δt is time delay, ρ_w is water density, k_p is the heat transfer coefficient between the pipes and the surroundings, D_p is the pipe diameter, T_∞ is the temperature of the material surrounding the pipes. This equation can be employed in the MILP model as long as the time discretization is sufficiently tight to capture the time delay in heat propagation (i.e. the time resolution has to be lower than the time the water needs to reach the closest building from the power plant). For this purpose, we considered a time resolution of 7.5 minutes in the case study.

2.8 Energy and comfort management strategies

In this work, the following three management strategies are considered and compared.

1. Reference management strategy: In the reference management strategy, the thermal power supplied to the buildings is regulated to maintain a set point in occupancy hours (20°C ±0.2°C during the heating season, and 25°C ±0.2°C during the cooling season) and units are switched off in non-occupancy hours (other than the advance needed to meet the setpoint at the first timestep of the day). The water delivery temperature of district heating network is adjusted linearly with outdoor air temperatureThe operational planning of the units (boilers, CHP engines, etc) is optimized using the MILP mode. Since the thermal power supplied to each building is not an optimization variable but fixed a -priori (no comfort management), this reference strategy is equivalent to applying the MES scheduling optimization approach originally proposed by Bischi et al. [3].
2. The "thermal comfort management (TCM) strategy": the end users of the buildings of the university are willing to participate a thermal comfort management program. Generally, the user who participates to demand side programs faces two types of discomfort: one due to timing, which occurs in household appliances, and the other linked to undesirable energy states (i.e. level of thermal comfort). In the present analysis, we consider only temperature dependence of users' comfort and the humidity is assumed to be controlled consequently by the air treatment unit. Comfort in mathematical modelling can be addressed by means of limit values to be met, or by penalties on deviation from the target condition to be included in the objective function with an appropriate weight. However, the inclusion of the comfort dimension in the objective function is limited by the subjectivity of the weight estimation [34]. Hence, we envisage a quality band of ±2°C around the setpoint (18 °C to 22 °C in the heating season and 23 °C to 27 °C in the cooling season), which is accepted a-priori by the users, and ASHRAE standards [35] constraints on ramps and drifts (Table 4) ensure smooth temperature variations. These constraints on comfort are imposed only in occupancy hours, while the building temperatures are not bound to meet any quality ranges in the rest of the day. Moreover, in the optimizations of energy district, water delivery temperature can vary and it can be used as a further source of flexibility. More specifically, we set an upper bound for the heating season (up to 90°C) and a lower bound for the cooling season (down to 7°C), while the limit in the other direction is driven by the

operation of the heat exchanger. As for the secondary circuit, we set the delivery temperature equal to the nominal value in occupancy hours to reduce the computational burden of the optimizations. This assumption can be made because the system shows already a degree of freedom to adjust heat supplied to the buildings, namely the bypass valve of the heat exchanger. Hence, in the TCM strategy, the building indoor temperatures, the thermal power supplied to each building and the DHN water temperatures (delivery and return) are included among the variables of the scheduling MILP (together with the commitment and load variables of the units). Given all of these degrees of freedom, the algorithm can either decide to reduce the heat requirements of buildings or to store heat in their mass (i.e. when there is availability of renewable sources or cogenerated heat).

3. The "Fixed Setpoint" (FS) strategy: it is an intermediate scenario, defined to assess to what extent the heat capacity of buildings and of the DHN can be exploited without the involvement of end-users. Thus, the profile of indoor temperature can be optimized only in non-occupancy hours, while water delivery temperature of the DHN as well as the operation of the units (boilers, CHP engines, etc) are optimized over the entire time horizon.

The main features of the operating strategies considered are summarized in Table 5Table 4.

Table 4 – ASHRAE Limits on temperature drifts and ramps [35]

Time Period	**0.25 h**	**0.5 h**	**1 h**	**2 h**	**4 h**
ΔT	1.1°C	1.7°C	2.2°C	2.8°C	3.3°C

Table 5– Fixed versus optimized variables in three operating strategies

	Indoor temperature non occupancy	Indoor temperature occupancy	Water delivery temperature (energy district)	Operation of MES units (boilers, CHP engines, etc)
Ref	FIXED	FIXED	FIXED	OPTIMIZED
FS	OPTIMIZED (unconstrained)	FIXED	OPTIMIZED (u.b. = 90°C DHN; l.b. = 7°C DCN)	OPTIMIZED
TCM	OPTIMIZED (unconstrained)	OPTIMIZED (±2°C)	OPTIMIZED (u.b. = 90°C DHN; ; l.b. = 7°C DCN)	OPTIMIZED

3. Case study

The presented model is applied to two different levels of spatial aggregation: firstly, we considered a single building not served by any district heating network but directly supplied by locally installed units, then the perspective is extended to several buildings located across a DHN. The optimizations have been formulated with Pyomo and the MILP has been solved with Gurobi solver [36]. To provide a broad applicability of the model, each optimization was carried out for three weeks of the year (representative of winter, mid-season and summer) and several different system architectures, described in detail in the following section. Regardless the operating strategy, thermal comfort requirements must be respected in all buildings from Monday to Friday from 8 a.m. to 6 p.m. The profiles of exogenous data used for the optimizations are depicted in Figure 4, for three different weeks of the year. The electrical demand generally spikes in the middle of the day, while a base load always occurs due to server's energy requirements. In all scenarios, the purchase price of electricity is the tri-hour tariff of non-domestic users in Italian protected market [37], while the sale price is provided by GME historical data [38]. It is worth to mention that the purchase price of natural gas is considered as constant over the time (40 €/MWh) and is derived from [39] on the basis of yearly average consumption of the university campus.

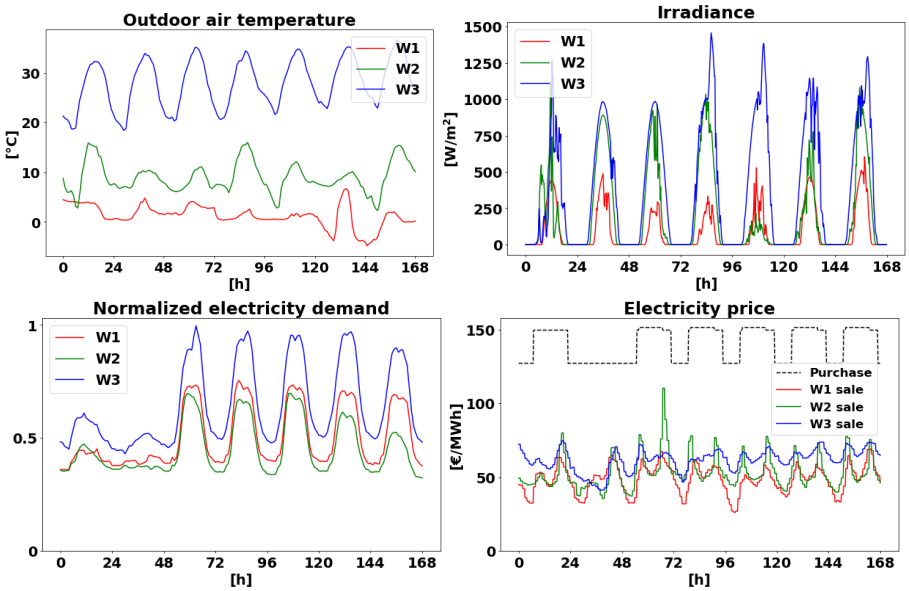

Figure 4 – Exogenous data profile from Saturday to Friday for three different weeks of the year (W1=winter; W2=spring; W3=summer).

3.1 MES designs

To provide an understanding of the effect of the thermal comfort management on MES operation and to potential savings in manifold applications, we extend the analysis to different technologies, summarized in Table 6.

Firstly, we applied the model to the current design of the energy system of the Campus of University of Parma, comprising boilers and compression chillers (CC). This configuration, referred to Design 1 (D1), is representative of the most traditional and widespread technology of DHN and DCN. Hence, we envisage a CCHP (Combined Cooling Heat and Power) energy system (Design 2), where the integration of the building thermal model in the optimization algorithm can unlock potential synergies among electric and thermal vectors. Design 3 (D3) comprises solar thermal collectors within the generation portfolio, while Design 4 (D4) encompasses photovoltaics panels, which can possibly feed the heat pump when the production outstrips the electricity demand of buildings. The choice of these two MES architecture was driven by the willing to investigate the role of buildings' load shifting capability in presence of renewable energy generation, as it might help to overcome the daily mismatch between supply and demand, which represents a major challenge especially in mid-season operation. Moreover, in order to respond to the current trend of fostering renewables, we envisage D3+ and D4+

scenarios, with high penetration of RES production (i.e. the roof surface employed is doubled).

The size of the units of each configuration are summarized in Table 6. The sizing criteria are the same for both single building and university campus application, but clearly the size of the system is scaled properly on the basis of the thermal requirements of the end-user. These criteria are as follows. As before mentioned, the first configuration (D1) is the current energy system supplying heat and cooling to the campus. Meanwhile, the internal combustion engine (ICE) employed in D2 covers 25% of heat peak, and the absorption chiller (AC) is sized accordingly. The ICE is undersized to avoid heat wasting in presence of an economic boost, while the residual demand is met by some auxiliary boilers and chillers. In design D3, solar thermal panels (ST) coupled with AC cover 50% of heat and cooling demand over the year, considering average efficiencies and irradiances. PV panels of D4 covers 25% of electricity demand over the year, while the HP meet half of the heat peak.

Table 6 – MES designs

	Description	Technology	Size (Single building)	Size (University Campus)
D1	Current design	Boiler	1050 kWth	2 x 7500 kWth
		CC	400 kWcool	4 x 1700 kWcool
D2	CCHP based design	Boiler	1050 kWth	3 x 4000 kWth; 1 x 3000 kWth
		ICE	150 kWel	2700 kWel
		CC	400 kWcool	4 x 1700 kWcool
		AC	160 kWcool	2000 kWcool
D3	ST based design	Boiler	1050 kWth	3 x 4000 kWth
		ST	125 kWth	1600 kWth
		CC	400 kWcool	4 x 1700 kWcool
		AC	95 kWcool	1200 kWcool
D3+	ST based design (with high RES penetration)	Boiler	1050 kWth	3 x 4000 kWth; 1 x 3000 kWth
		ST	300 kWth	3200 kWth
		CC	400 kWcool	4 x 1700 kWcool
		AC	190 kWcool	2400 kWcool
D4	PV based design	Boiler	2 x 530 kWth	3 x 4000 kWth
		HP	530 kWth	6000 kWth
		PV	195 kWel	2500 kWel
		CC	400 kWcool	4 x 1700 kWcool
D4+	PV based design (with high RES penetration)	Boiler	2 x 530 kWth	3 x 4000 kWth
		HP	530 kWth	6000 kWth
		PV	195 kWel	5000 kWel
		CC	400 kWcool	4 x 1700 kWcool

3.2 Buildings and distribution system features

Single building

The building under investigation, here referred to B0, is a two-floor building of Campus of University of Parma, with surface/volume of 53% and time-constant τ (defined in 2.4) of 34 hours. Optimizations are also performed for two fictitious buildings featuring one different thermal property (respectively inertia and window surface) with respect to B0: B1, representing a heavy building with τ of 158 h, and B2, featuring a larger glazed surface (the triple of B0). These buildings thermal properties, summarized in Table 7,

have been chosen so that they are representative of the diversity of the buildings of the university campus.

Table 7 – Buildings construction parameters

	τ [h]	C_k [kWh/°C]	UA [kW/°C]	$mc_{p,k}^{nat}$ [kW/°C]	$mc_{p,k}^{force}$ [kW/°C]	Window surface [m²]
B0	34	282.5	6.89	1.52	7.62	55
B1	158	1328.5	6.89	1.52	7.62	55
B2	34	282.5	6.89	1.52	7.62	146

University campus

The energy district of the Campus of the University of Parma includes 12 buildings with different thermal properties, which will influence the optimal indoor temperature evolution. Indeed, the area to volume ratio of the buildings varies from 33% to 55%, whereas the time-constant ranges from 34 h to 158 h. The DHN presents a radial topology with buildings fairly equidistant from the power plant (450 m) and the water flows in the primary loop with an average speed of 1 m/s. The design delivery and return temperatures of the DHN primary loop are 90 °C and 55 °C, while 50 °C (delivery) and 40°C (return) for the secondary loop. When operating in the cooling mode (summer season), the delivery and return temperatures of the primary loop are 7 °C and 12 °C respectively, while 9°C and 17°C in the secondary loop. It is worth noting that in the heating mode the flow with larger heat capacity rate (product of mass flow rate and specific heat capacity) is the secondary loop, while it becomes the primary loop in the cooling mode. This change is considered by the heat exchanger model presented in Section 2.7

4. Results

In this section, the main results of the test cases are analyzed, in terms of the unit commitment, buildings and DHN temperature profiles. For each MES configuration, the advantages of TCM (and of the intermediate FS) are compared with the reference strategy, first at single building level and then the focus is shifted to the energy district. The analysis also provides an insight into the different thermal behavior of buildings with diverse construction properties. In particular, the outcomes of single-building optimizations are firstly discussed for the reference building B0, and then they are compared with that of the buildings B1 and B2, featuring respectively a higher time constant and a larger glazed area.

The comparison is carried out from both a technical and an economic perspective and the main highlights of the effect of the management strategies are summarized in Table 8, in

terms of generators performances, savings on total operating costs and renewable energy exploitation. A more detailed picture of operational cost savings (Table 9) is provided at the end of the section, encompassing all optimized scenarios.

Table 8 – Comparison of generators performances, operating cost and renewable exploitation of the three management strategies (Ref, FS and CM) for the most relevant scenarios of the case study (W1 = winter, W2 = spring, W3 = summer).

	D1			D2		D3	D4+
	η boiler (W1)	**COP CC (W3)**	**Average purchase price [€/MWh$_{el}$] (W3)**	**Operating cost [€/w] (W1)**	**Operating cost [€/w] (W3)**	**% ST dissipated (W2)**	**% extra PV sold (W2)**
B0							
Ref	88.1%	3.3	151	3875	4769	74%	73%
FS	88.1%	3.5	148	2821	4530	27%	58%
CM	92.1%	3.8	138	2707	4266	1%	34%
B1							
Ref	92.0%	3.6	150	3872	4725	47%	70%
FS	92.0%	3.7	143	2793	4482	20%	29%
CM	93.7%	4.3	127	2664	4208	1%	19%
Campus							
Ref	91.4%	3.4	150	46586	61232	82%	84%
FS	93.0%	3.7	146	26829	49165	32%	39%
CM	93.2%	4.2	136	26600	38776	8%	38%

Using a standard laptop computer (Intel i7-5500U @ 2.40 GHz, 8 GB RAM), solving the single-building cases over one week time horizon with 15 minutes of time steps need a computational time of less than 5 minutes, while solving the campus case study over one week and a time step of 7.5 minutes needs approximately 5 hours. This computational times are good for the large size of the MILP problems: as an example, the campus case study with D1 winter configuration features 250160 continuous variables, 6725 binary variables and 384059 constraints. An important time saving can be obtained by shortening the time horizon modelled in the MILP: if the optimization horizon is shortened to three days (minimum to exploit the heat capacity of the buildings), solving the campus case study takes only 20 minutes.

DESIGN 1

Single building

Design 1 represents the most traditional solution adopted to provide cooling and heating services to buildings. With this MES configuration (Figure 5) , TCM takes advantage of the heat capacity of buildings to enhance machines performance, notably exploiting the lower interval of the comfort range in winter (week W1) and the entire range in summer (week W3).

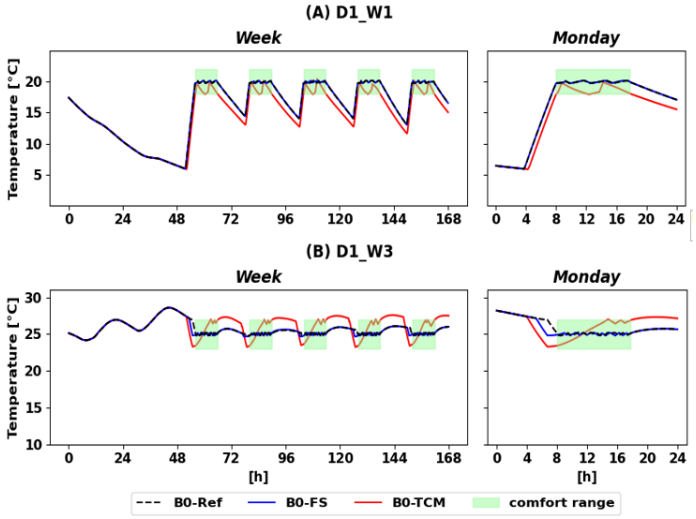

Figure 5. Indoor temperature profiles (Saturday-Friday) of the building B0, with the reference Ref (black-dashed), intermediate FS (blue) and thermal comfort management TCM (red) strategy. The profiles refer to MES configuration D1 during winter week W1 (Fig. A) and summer week W3 (Fig. B).

Hence, TCM reduces the switching on/off and the operation at partial loads of the boiler, improving its mean efficiency from 88.1% in B0-Ref to 92.1% in B0-TCM (Table 8). The algorithm advances the chiller operation and overcools the buildings down to 23°C in the early morning, to benefit from COP improvement at lower external temperatures and to buy cheaper electricity. Indeed, mean COP improves from 3.3 in B0-Ref to 3.8 in B0-TCM, while average electricity price decreases from 151 €/MWh to 138 €/MWh (Table 8). The intermediate strategy FS (in which heat capacity of buildings is exploited only in non-occupancy hours) has no effect on boiler commitment, while the advance of compression chiller startup slightly improves mean COP (to 3.5 in B0-FS) and decreases mean electricity purchase price (to 148 €/MWh in B0-FS). From an economic perspective, in B0-TCM total operating costs (machines consumption + O&M) are reduced in winter by 14.5% and in summer by 30.6% (Table 9). Obviously, a fraction of

these savings is imputable to lower heating/cooling requirements of the building (due to decrease/increase of indoor temperature). When comparing the three buildings considered (see Table 8 and Table 9) in it can be noticed that building B1 (with larger time constant) shows higher savings (up to 56%) and larger average COP (equal to 4.3) with the TCM strategy in the summer mode. This difference between buildings occurs in all scenarios where shifting production plays a pivotal role in the optimization and an understanding of this behavior will be provided in the discussion of design D3 results.

University campus

In the case study of the university campus, the optimization of water delivery temperature reduces the heat losses across the distribution system. Nevertheless, they represent only a small fraction of heat produced by generators, since the pipes are considered as well-insulated, and the estimated heat losses in the benchmark might be lower using a slightly different OAT function. A more remarkable advantage of the optimization is that heat can be stored and released in the short term in the distribution system by adjusting water delivery temperature. The amount of this storable energy depends on the heat capacity of the distribution network and on the range of temperature available. As the heat capacity of the distribution system represents only a small fraction (2%) of that of the buildings, the role of allowable temperature variation is of major importance. Consequently, the flexibility provided by the distribution system differs significantly between the winter and the summer case, as water primary delivery temperature of DHN can vary between 90°C and slightly above the temperature of the secondary loop (50°C), while in DCN this interval is only of few degrees. This different behaviour characterizing the DHN and the DCN can be noticed in

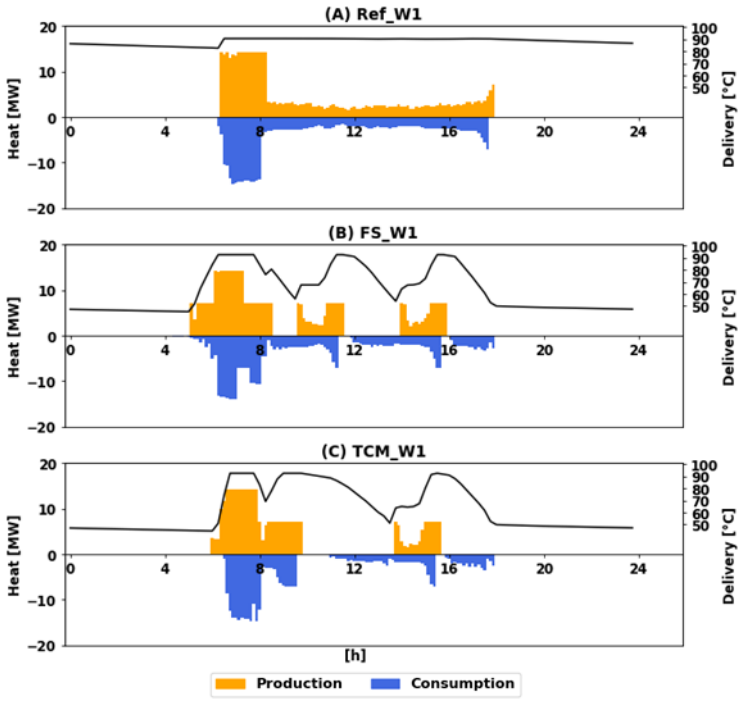

Figure 6 and Figure 7, where the profiles of the thermal power produced by the generators and that delivered to the buildings by fan-coil units are depicted (together with the

evolution of primary delivery temperature). A temporal decoupling between heat production and consumption occurs in FS and TCM strategies, thanks to the variation of DHN water delivery temperature, allowing for machine efficiency improvement. Meanwhile, the load shifting capability provided by DCN is very limited and the profiles of production and consumption are very similar over time.

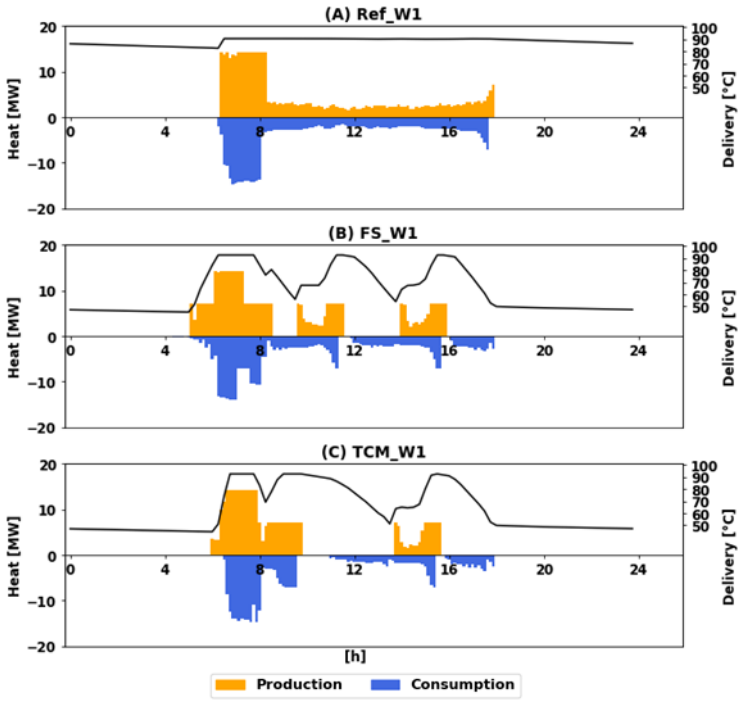

Figure 6 - Daily profiles of heat produced by generators (orange), heat delivered to the buildings by the fan-coil units (blue), delivery temperature (black) of the primary loop of the DHN, with three different strategies, namely reference Ref (Fig. A), intermediate FS (Fig. B) and thermal comfort management TCM (Fig. C). The profiles refer to MES configuration D1 in a winter day (week W1)

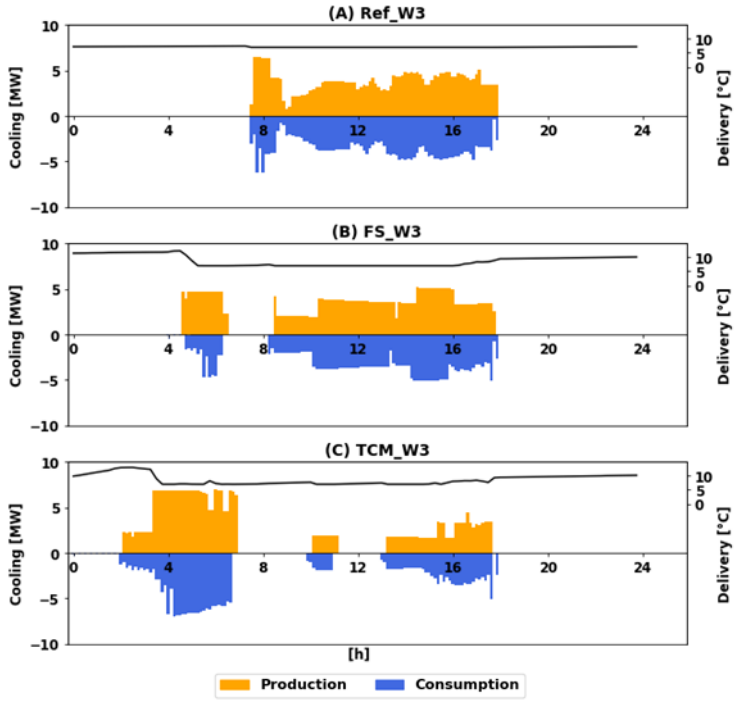

Figure 7 - Daily profiles of cooling power produced by generators (orange), cooling delivered to the buildings by the fan-coil units (blue), delivery temperature (black) of the primary loop of the DCN, with three different strategies, namely reference Ref (Fig. A), intermediate FS (Fig. B) and thermal comfort management TCM (Fig. C). The profiles refer to MES configuration D1 in a summer day (week W3).

The comparison of the three strategies is provided by Table 8. The only optimization of DHN water delivery temperature (FS) is sufficient to improve machines performance in and the further possibility to store heat in building mass does not provide any benefit from a technical point of view in winter. Conversely, the employment of heat capacity of buildings (TCM) in summer enhances the mean COP of chillers from 3.4 (Ref) to 4.2 and reduces average electricity purchase price from 150 (Ref) to 136 €/MWh, while with FS these values are of 3.7. and 146 €/MWh, respectively.

DESIGN 2

Single building

Design 2 is CCHP configuration, where the engine is under sized with respect to heating and cooling requirements. It might be representative of situations in which heat produced by the engine can never be dissipated, i.e. in the attempt to participate to white certificate market (but the effect of possible incentives is not taken into account in this analysis, so not to lose generality). In the optimized strategies, both TCM and FS, the engine follows the electrical load to maximize the self-produced electricity (**Errore. L'origine riferimento non è stata trovata.**), which would be otherwise purchased at expensive tariff from the national grid, and the building is heated (or cooled) accordingly (

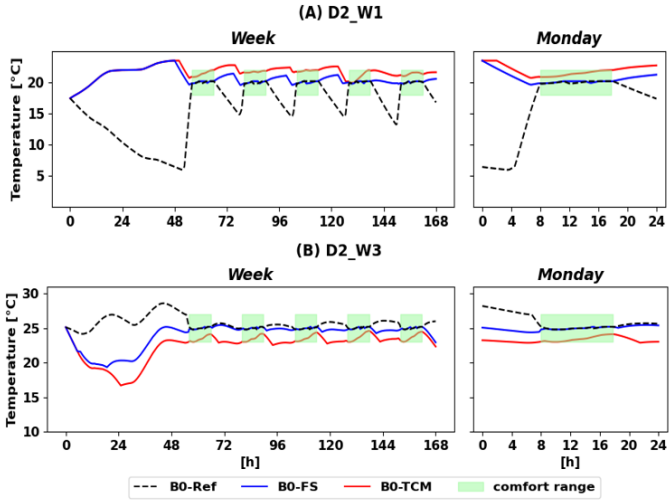

Figure 8).

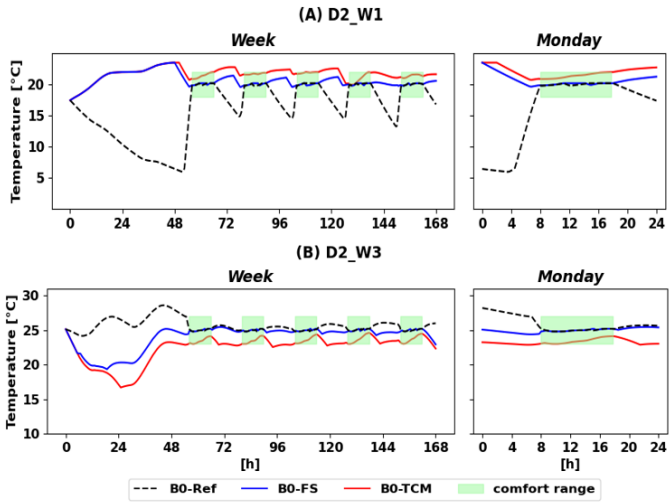

Figure 8. Indoor temperature weekly profiles (Saturday-Friday) of the building B0, with the reference Ref (black-dashed), intermediate FS (blue) and thermal comfort management TCM (red) strategy. The profiles refer to MES configuration D2 during winter week W1 (Fig. A) and summer week W3 (Fig. B).

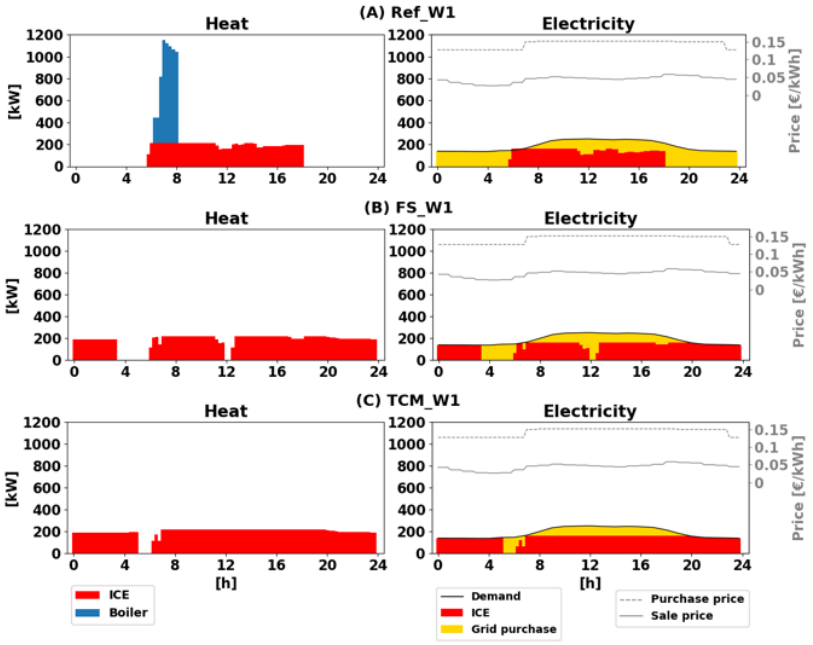

Figure 9 – Daily profile of the unit commitment and the grid exchange of the building B0, with the reference Ref (Fig. A), intermediate FS (Fig. B) and thermal comfort management TCM (Fig. C) strategy. The profiles refer to MES configuration D2 during winter week W1.

The ICE, although undersized, meets the entire thermal demand without the auxiliary boiler (**Errore. L'origine riferimento non è stata trovata.**), since it runs continuously even in non-occupancy hours following the electrical base load. Despite the increase of energy delivered to the building, operating costs (including the net exchange with the grid) are significantly reduced in winter by 27% in B0-FS and 30% in B0-TCM (Table 8). In this case, the flexibility provided by the inclusion of the building model in the MILP algorithm (rather considering thermal demand as exogenous) is remarkably exploited also in non-occupancy hours. Nevertheless, this result is strictly related to the shape of the electrical demand profile under investigation and this consideration might not be valid in different situations. The difference in savings between buildings are negligible.

University campus

The optimization of the energy district management, similarly to single-building test cases, aims at increasing self-produced electricity by the engine. To this end, the algorithm can shape the profile of water delivery temperature of the DHN. The electricity

bought from the grid is therefore reduced with FS and TCM (in winter) and decreasing operating costs by respectively 42.4% and 42.9% compared to the benchmark (Table 8).

DESIGN 3

Single building

Design D3 features solar thermal collectors coupled with an absorption chiller (plus auxiliary boiler and CC). Under this MES architecture, TCM strategy results particularly interesting when RES availability mismatches thermal demand. As a matter of fact, in spring scenario, the optimal indoor temperature of the building hits a peak in the middle of the day and then it decreases, thus reducing from 74% (B0-Ref) to 1% (B0-TCM) the amount of dissipated ST production and decreasing total operating costs (fuel + O&M) by 40.8%. These savings are more pronounced in the building B1, as it can be noticed in Table 9. Indeed, the higher time constant characterizing this building affects the temperature profile, which is generally smoother than in B0 and B2 (Figure 10), and this allows to shift more the production without jeopardizing users comfort.

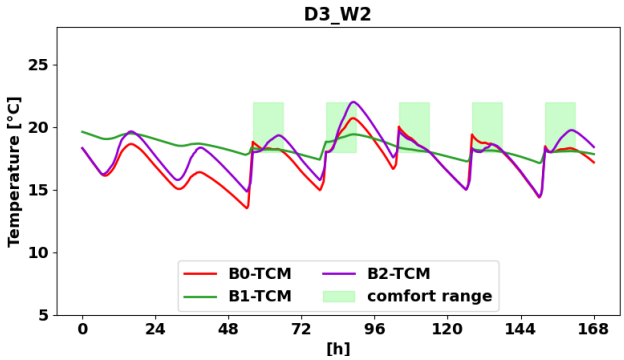

Figure 10. Indoor temperature weekly profiles (Saturday-Friday) of the buildings B0 (red), B1 (green) and B2 (purple), with thermal comfort management TCM strategy. The profiles refer to MES configuration D3 in spring week W2.

University campus

The optimization of primary water delivery temperature has no effect on the exploitation of solar production, since the collectors directly supply the secondary loop of the buildings and, as before mentioned, we set delivery temperature of the secondary loop equal to the nominal value in occupancy hours. This assumption is mainly driven by the concern to reduce the computational time, considering that in any case heat transferred to buildings can be regulated by means of the bypass valve. Therefore, given these assumptions, the role of the heat capacity of buildings is of major importance. Indeed,

when there is abundancy of ST production (i.e. mid-season) TCM allows to save 61.5% on fuel and O&M in spring scenario, decreasing the percentage of dissipated RES production from 82% to 8% (see Table 8). In the intermediate strategy FS, costs are reduced by 30.0% thanks to the possibility to store ST heat produced in non-occupancy hours (i.e. during weekends) in buildings thermal mass, which would be otherwise dissipated in benchmark scenario.

DESIGN 4

Single building

Design D4 features a heat pump with an auxiliary boiler, photovoltaics panels and a compression chiller. In winter, the heat pump is rarely employed, because of COP reduction with external temperatures. Thus, the considerations of design D1 are also valid for this MES configuration. Nevertheless, it is worth to analyse the employment of TCM when PV outstrips electrical demand, such as in spring scenario when large PV power is installed (D4+). In this case, with TCM, indoor temperature of the building rises in the middle of the day and therefore a greater fraction of the excess PV production – 66% in B0-TCM instead of 27% in B0-Ref (Table 8)– can be supplied to HP instead of being sold (at low price) to the grid. This positively affects operating costs which are reduced by 8.4% in B0-TCM, reaching 14.6% in B1-TCM. Meanwhile, costs reduction of the intermediate strategy FS (in the order of magnitude of 3% in B0) are related to the possibility to use the surplus of PV production occurring at the weekend to overheat the buildings, since the indoor temperature is free to vary in non-occupancy hours.

University Campus

Similarly to single-building optimizations, the flexibility provided by the heat capacity of the system (both DHN and buildings) is effective to overcome the issue of daily mismatch between RES availability and thermal demand.

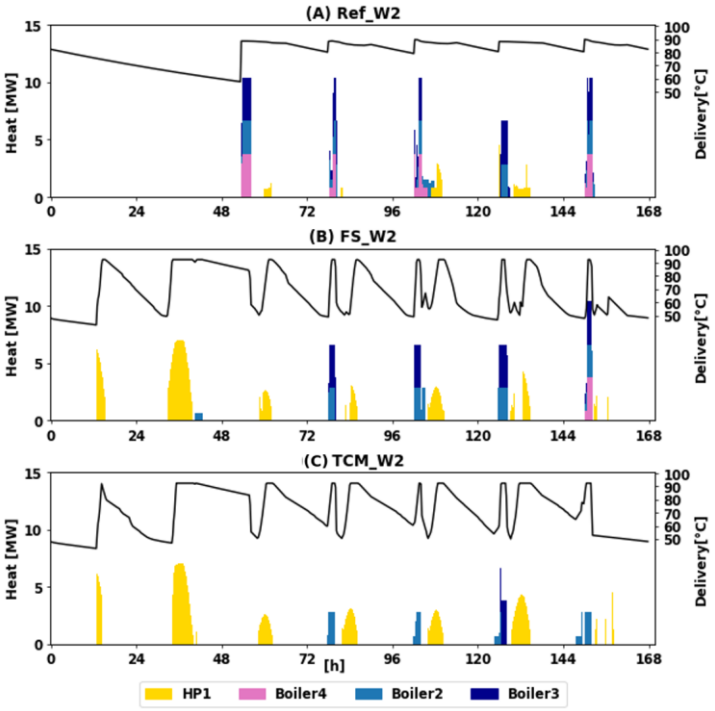

Figure 11 depicts the unit commitment of thermal generators and the evolution of DHN supply temperature in the three management strategies, under D4+ spring scenario. The optimized delivery temperature rises in the presence of RES, when PV production supplies the HP, while it drops in the rest of the day. As a result, the share of excess PV production sold to the grid (at low price) is reduced from 84% in the reference strategy to 39% with FS and 38% with TCM. Hence, given the assumptions in this case study about the allowable range of the delivery temperature, renewable sources exploitation can be notably increased by only optimizing water delivery temperature. Figure 12 highlights the different thermal behavior of two buildings of the campus, featuring a high and a low time constant. It is possible to notice that TCM exploits the entire quality band (both upward and downward) available in occupancy hours, but temperature variations are more pronounced in building with low τ. Total operating costs are positively affected by the optimization and, as shown in Table 9, the savings of TCM compared to the reference scenario are 21.6% in D4+-spring, while costs reduction of FS are of 4.6%.

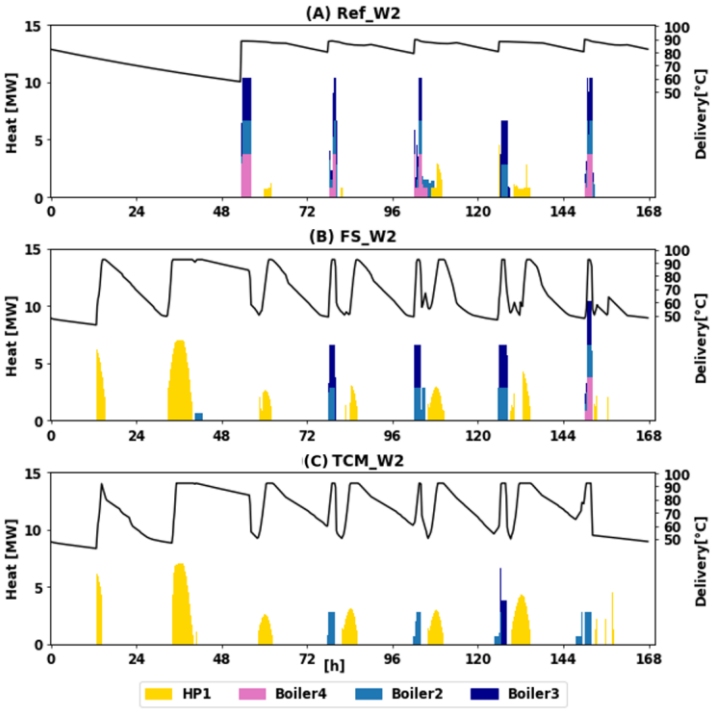

Figure 11. Unit commitment and DHN delivery temperature weekly profiles (Saturday-Friday), with three different strategies, namely reference Ref (Fig. A), intermediate FS (Fig. B), and thermal comfort management TCM (Fig. C). The profiles refer to MES configuration D4+ in spring week W2.

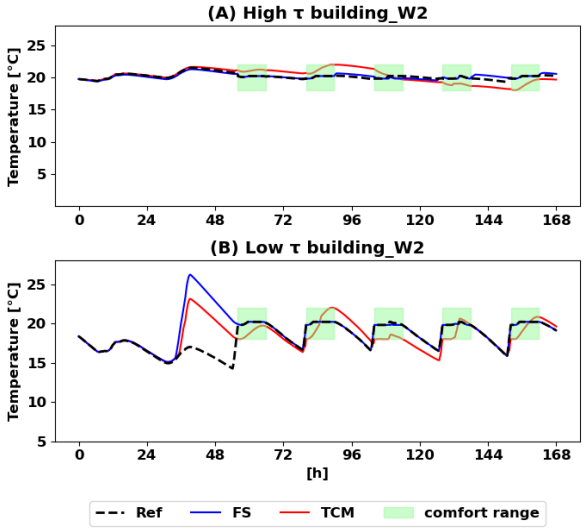

Figure 12. Indoor temperature weekly profiles (Saturday-Friday) of two reference buildings of the university campus featuring a high (Fig. A) and a low time constant τ (Fig. B), with reference Ref (black-dashed), intermediate FS (blue) and thermal comfort management TCM (red) strategy. The profiles refer to MES configuration D4+ during spring week W2.

Table 9 – Total operating costs variation of strategies FS and TCM with respect to the reference strategy (Ref) in building B0, B1 and B2 and in the university campus, for various MES configurations and weeks of the year (W1=winter; W2=spring; W3=summer).

		B0		B1		B2		University Campus	
Design	**Week**	**FS**	**TCM**	**FS**	**TCM**	**FS**	**TCM**	**FS**	**TCM**
D1	W1	0%	-14.5%	0%	-18.3%	0%	-16.3%	-2.6%	-14.4%
	W2	0%	-35.6%	0%	-32.1%	0%	-36.0%	-27.5%	-48.0%
	W3	-4.4%	-30.6%	-5.3%	-56.4%	-3.8%	-21.9%	-6.1%	-26.4%
D2	W1	-27.2%	-30.1%	-27.9%	-31.2%	-26.4%	-29.8%	-42.4%	-42.9%
	W2	-17.3%	-22.4%	-17.1%	-23.3%	-17.4%	-21.0%	-31.3%	-40.5%
	W3	-5.0%	-10.6%	-5.1%	-10.9%	-8.2%	-18.3%	-19.7%	-36.7%
D3	W1	-1.7%	-18.0%	-3.7%	-21.4%	-0.9%	-17.9%	-15.0%	-26.4%
	W2	-5.5%	-40.8%	-10.5%	-48.2%	-6.4%	-44.0%	-30.0%	-61.5%
	W3	-9.1%	-52.5%	-15.7%	-80.2%	-4.5%	-31.2%	-20.1%	-44.9%
D3+	W1	-2.0%	-21.0%	-3.2%	-21.6%	-2.1%	-20.8%	-5.5%	-21.9%
	W2	-12.5%	-53.8%	-23.7%	-82.1%	-17.3%	-60.2%	-20.1%	-44.9%
	W3	-20.5%	-74.1%	-43.9%	-83.6%	-16.9%	-53.6%	-37.4%	-67.2%
D4	W1	0%	-2.1%	0.0%	-4.0%	0%	-2.3%	-0.3%	-2.8%
	W2	0%	-2.8%	0.0%	-4.9%	0%	-2.7%	-4.4%	-19.9%
	W3	0%	-2.9%	0%	-5.5%	0%	-2.8%	-3.3%	-7.6%
D4+	W1	0%	-2.3%	0.0%	-3.9%	0%	-2.4%	-0.3%	-2.8%
	W2	-2.9%	-8.4%	-7.4%	-14.6%	-2.9%	-5.8%	-4.6%	-21.6%
	W3	-0.9%	-5.4%	-2.1%	-9.1%	-1.7%	-5.3%	-1.7%	-7.6%

5. Conclusions and future works

This work tackles the optimization of the operation planning of a Multi Energy System and thermal comfort management in buildings. A linearized thermal model of the building is included in the MILP formulation, so that the thermal demand of buildings becomes a variable to optimize, together with the evolution of their indoor temperature, the commitment and the load variables of the energy generators.

The proposed method is firstly applied to single building test cases encompassing a wide range of possible applications in terms of thermal features of the building (thermal inertia and window surface) and design of the energy system supplying heating, cooling and electricity (solar panels, boiler, heat pumps, internal combustion engines). At this stage

of the analysis, the building is supposed to be served by locally installed units without a centralized district heating network.

The advantage of optimizing also thermal comfort in addition to the operation of the generation units is determined by comparing the reference management strategy of Parma University Campus with the so-called “thermal comfort management” (TCM). In this scenario, the energy service company requires the users to accept a variation of ±2°C around the setpoint. The possibility to exploit the heat capacity of buildings improves overall performance and reduces operating costs. In particular, thermal comfort management has proven to be a viable option for increasing renewable energy exploitation, when the production mismatches the demand, and for shifting production to low electricity price periods. The building with higher time constant (defined in 2.4) exhibits smoother temperature fluctuations and thermal comfort management allows for greater savings in this type of buildings especially when the optimization leverages on production shifting. In combined heat and power (and cooling) configurations, the embedding of building model in the MILP formulation enables a more flexible operation of the internal combustion engine. Considered the shape of the electrical load of the case study, the optimal solution for the engine is to follow the electric load and heat (or cool) buildings accordingly.

To assess the extent to which the heat capacity of buildings can be exploited without the involvement of end-users, we compared thermal comfort management with an intermediate management strategy, "Fixed Setpoint" (FS), in which indoor temperature profile of buildings is only optimized during non-occupancy hours. The results show that, given the shape of the electric load of the case study under investigation(Figure 8), the fixed setpoint strategy significantly reduces the operating costs in presence of an internal combustion engine, because it allows the generator to follow electrical demand when buildings are not occupied. Meanwhile, the thermal comfort management strategy allows optimizing also the performance of the machines and the exploitation of renewables.

Subsequently, the methodology is further extended to apply the model to an energy district. In this framework, a simplified linear representation of the district heating network is included to account for the delay in heat propagation and optimize the operation of the generators with higher accuracy. This method is implemented on the Campus of University of Parma (over different multi energy system designs), where water delivery temperature is currently adjusted as a linear function of outdoor air temperature. We compare this reference management with the two proposed strategies, FS and TCM, which can rely on an additional source of flexibility, namely the water delivery

temperature. Indeed, energy can be stored/released in the short term in the district heating network by increasing/decreasing this temperature. The amount of the "storable energy" depends on the heat capacity of the distribution network, which is approximately 2% of that of the buildings, and on the available temperature interval to the optimization. As a result, given the assumptions on the allowable water temperature variation of the case study, the optimization of the flow temperature can improve the performance of the generators and the use of renewable energy in district heating network, while this is not the case in district cooling network, where water delivery temperature is less free to vary. The proposed MILP method appears to be an interesting option not only for operational planning, but also to manage comfort in buildings and it could be integrated into rolling horizon algorithms today used for optimizing the energy management strategy of multi-energy systems and energy districts. Further extensions of the methodology might involve more detailed models of the buildings and thermal energy comfort, as well as extending the optimization formulation to deal with forecast uncertainty. Moreover, the performance curves of the machines can be refined to include the effect of delivery temperature variation.

References

[1] P. Mancarella, "MES (multi-energy systems): An overview of concepts and evaluation models," *Energy*, vol. 65, pp. 1–17, 2014, doi: 10.1016/j.energy.2013.10.041.

[2] D. Ürge-Vorsatz, L. F. Cabeza, S. Serrano, C. Barreneche, and K. Petrichenko, "Heating and cooling energy trends and drivers in buildings," *Renew. Sustain. Energy Rev.*, vol. 41, pp. 85–98, 2015, doi: 10.1016/j.rser.2014.08.039.

[3] A. Bischi *et al.*, "A detailed MILP optimization model for combined cooling, heat and power system operation planning," *Energy*, vol. 74, no. C, pp. 12–26, 2014, doi: 10.1016/j.energy.2014.02.042.

[4] L. Moretti, G. Manzolini, and E. Martelli, "MILP and MINLP models for the optimal scheduling of multi-energy systems accounting for delivery temperature of units, topology and non-isothermal mixing," *Appl. Therm. Eng.*, vol. 184, no. September 2020, p. 116161, 2021, doi: 10.1016/j.applthermaleng.2020.116161.

[5] L. Taccari, E. Amaldi, E. Martelli, and A. Bischi, "Short-Term Planning of Cogeneration Power Plants: a Comparison Between MINLP and Piecewise-Linear MILP Formulations," in *12 International Symposium on Process Systems Engineering and 25 European Symposium on Computer Aided Process Engineering*, vol. 37, K. V Gernaey, J. K. Huusom, and R. B. T.-C. A. C. E. Gani, Eds. Elsevier, 2015, pp. 2429–2434.

[6] F. Brahman, M. Honarmand, and S. Jadid, "Optimal electrical and thermal energy management of a residential energy hub, integrating demand response and energy storage system," *Energy Build.*, vol. 90, pp. 65–75, 2015, doi: 10.1016/j.enbuild.2014.12.039.

[7] D. Buoro, P. Pinamonti, and M. Reini, "Optimization of a Distributed Cogeneration System with solar district heating," *Appl. Energy*, vol. 124, pp. 298–308, 2014, doi: 10.1016/j.apenergy.2014.02.062.

[8] A. Gambarotta, M. Morini, N. Pompini, and P. R. Spina, "Optimization of load allocation strategy of a multi-source energy system by means of dynamic programming," *Energy Procedia*, vol. 81, no. March 2016, pp. 30–39, 2015, doi: 10.1016/j.egypro.2015.12.056.

[9] V. Marano, G. Rizzo, and F. A. Tiano, “Application of dynamic programming to the optimal management of a hybrid power plant with wind turbines, photovoltaic panels and compressed air energy storage,” *Appl. Energy*, vol. 97, pp. 849–859, 2012, doi: 10.1016/j.apenergy.2011.12.086.

[10] T. Fang and R. Lahdelma, “Genetic optimization of multi-plant heat production in district heating networks,” *Appl. Energy*, vol. 159, pp. 610–619, 2015, doi: 10.1016/j.apenergy.2015.09.027.

[11] B. Huang, Y. Wang, C. Yang, Y. Li, and Q. Sun, “A neurodynamic-based distributed energy management approach for integrated local energy systems,” *Int. J. Electr. Power Energy Syst.*, vol. 128, no. June, p. 106737, 2021, doi: 10.1016/j.ijepes.2020.106737.

[12] L. Yushuai, W. Gao, W. Gao, H. Zhang, and J. Zhou, “A Distributed Double-Newton Descent Algorithm for Cooperative Energy Management of Multiple Energy Bodies in Energy Internet,” *IEEE Trans. Ind. Informatics*, 2020 (In press), doi: 10.1109/tii.2020.3029974.

[13] G. Sandou, S. Font, S. Tebbani, A. Hiret, and C. Mondon, “Predictive Control of a Complex District Heating Network,” no. May 2014, 2006, doi: 10.1109/CDC.2005.1583351.

[14] L. Moretti, E. Martelli, and G. Manzolini, “An efficient robust optimization model for the unit commitment and dispatch of multi-energy systems and microgrids,” *Appl. Energy*, vol. 261, no. December 2019, p. 113859, 2020, doi: 10.1016/j.apenergy.2019.113859.

[15] G. Darivianakis, A. Georghiou, R. S. Smith, and J. Lygeros, “A stochastic optimization approach to cooperative building energy management via an energy hub,” *Proc. IEEE Conf. Decis. Control*, vol. 54rd IEEE, no. Cdc, pp. 7814–7819, 2015, doi: 10.1109/CDC.2015.7403455.

[16] G. Darivianakis, A. Georghiou, R. S. Smith, and J. Lygeros, “The Power of Diversity: Data-Driven Robust Predictive Control for Energy-Efficient Buildings and Districts,” *IEEE Trans. Control Syst. Technol.*, vol. 27, no. 1, pp. 132–145, 2019, doi: 10.1109/TCST.2017.2765625.

[17] F. J. Baader, M. Mork, A. Xhonneux, D. Müller, A. Bardow, and M. Dahmen, “Mixed-Integer Dynamic Scheduling Optimization for Demand Side Management,” *Proc. 30th Eur. Symp. Comput. Aided Process Eng.*, 2020.

[18] I. Duong Tung Nguyen and Long Bao Le, Senior Member, “Joint Optimization of Electric Vehicle and Home Energy Scheduling Considering User Comfort Preference,” *IEEE Trans. Smart Grid*, vol. 5, no. 1, 2014, doi: 10.1108/NFS-04-2016-0042.

[19] E. Guelpa, S. Deputato, and V. Verda, “Thermal request optimization in district heating networks using a clustering approach,” *Appl. Energy*, vol. 228, no. July, pp. 608–617, 2018, doi: 10.1016/j.apenergy.2018.06.041.

[20] W. Gu, J. Wang, S. Lu, Z. Luo, and C. Wu, “Optimal operation for integrated energy system considering thermal inertia of district heating network and buildings,” *Appl. Energy*, vol. 199, pp. 234–246, 2017, doi: 10.1016/j.apenergy.2017.05.004.

[21] C. Saletti, A. Gambarotta, and M. Morini, “Development, analysis and application of a predictive controller to a small-scale district heating system,” *Appl. Therm. Eng.*, vol. 165, no. August 2019, p. 114558, 2020, doi: 10.1016/j.applthermaleng.2019.114558.

[22] M. Zatti, M. Gabba, M. Rossi, M. Morini, A. Gambarotta, and E. Martelli, “Towards the optimal design and operation of multi-energy systems: The ‘efficity’ project,” *Environ. Eng. Manag. J.*, vol. 17, no. 10, pp. 2409–2419, 2018, doi: 10.30638/eemj.2018.239.

[23] “Jehnbacher.” 2016.

[24] F. W. Yu and K. T. Chan, “Optimum load sharing strategy for multiple-chiller systems serving air-conditioned buildings,” *Build. Environ.*, vol. 42, no. 4, pp. 1581–1593, 2007, doi: 10.1016/j.buildenv.2006.01.006.

[25] Broad, “BROAD X Non-electric Chiller: Model Selection & Design Manual,” 2008, [Online]. Available: http://www.broadusa.net/en/wp-content/uploads/2015/03/Broad-X-chiller-Model-selection-design-manual-C.pdf.

[26] P. Rivière, J. Adnot, D. Marchio, L. Pérez-Lombard, and J. Ortiz, “A method to reduce European chiller hourly load curves to a few points.,” Feb. 2005.

[27] R. K. Johnson, “Measured Performance of a Low Temperature Air Source Heat Pump,” no. September, 2013.

[28] "PowerLink Power Systems," 2015. https://www.powerlinkenergy.com/.
[29] EN 14825, "Air conditioners, liquid chilling packages and heat pumps, with electrically driven compressors for space heating and cooling - Testing and rating at part load conditions and calculation of seasonal performance," vol. 44, no. 0, 2013.
[30] "Mitsubishi Electric-Solar Innovations." 2000.
[31] X. Li and J. Wen, "Review of building energy modeling for control and operation," *Renew. Sustain. Energy Rev.*, vol. 37, pp. 517–537, 2014, doi: 10.1016/j.rser.2014.05.056.
[32] A. Gambarotta, M. Morini, M. Rossi, and M. Stonfer, "A Library for the Simulation of Smart Energy Systems: The Case of the Campus of the University of Parma," *Energy Procedia*, vol. 105, pp. 1776–1781, 2017, doi: 10.1016/j.egypro.2017.03.514.
[33] L. Dobos, J. Jäschke, H. Mordt, S. Skogestad, and S. Narasimhan, "Dynamic Model and Control of Heat Exchanger Networks," *Nt.Ntnu.No*, vol. 37, no. June 2014, pp. 37–49, 2009, [Online]. Available: http://home.nt.ntnu.no/users/skoge/diplom/prosjekt07/smedsrud/HelSmRapp07.doc.
[34] R. Lahdelma and H. Hakonen, "An efficient linear programming algorithm for combined heat and power production," *Eur. J. Oper. Res.*, vol. 148, no. 1, pp. 141–151, 2003, doi: 10.1016/S0377-2217(02)00460-5.
[35] "ASHRAE STANDARD 55-2004. Thermal Environmental Conditions for Human Ocupancy," 2004, doi: 10.1007/0-387-26336-5_1680.
[36] "GUROBI." http://www.gurobi.com.
[37] "Servizio elettrico nazionale." https://www.servizioelettriconazionale.it/it-IT/tariffe/altri-usi/bta-6-trioraria.
[38] "GME." https://www.mercatoelettrico.org/it/Statistiche/ME/DatiSintesi.aspx.
[39] ARERA, "Prezzi finali del gas naturale per i consumatori industriali - UE e area Euro." https://www.arera.it/it/dati/gpcfr2.htm.